

Electronic Supplementary Information

Dopant-Free Organic Hole Transport Material for Efficient Planar Heterojunction Perovskite Solar Cells

Yongsheng Liu,^{a,b} Qi Chen,^{a,b} Hsin-Sheng Duan,^{a,b} Huanping Zhou,^{a,b} Yang (Michael) Yang,^a Huajun Chen,^a Song Luo,^{a,b} Tze-Bin Song,^{a,b} Letian Dou,^{a,b} Ziruo Hong^a and Yang Yang^{*a,b}

^aDepartment of Materials Science and Engineering, University of California, Los Angeles, California 90095, USA

^bCalifornia NanoSystems Institute, University of California, Los Angeles, California 90095, USA

Materials

Hydroiodic acid (sigma, 57 wt %), DMF (Sigma Aldrich, 99%), lead(II) chloride (Sigma-Aldrich, 98%), methylamine (Sigma Aldrich, 33 wt % in absolute ethanol), titanium diisopropoxide bis(acetylacetonate) ($[(\text{CH}_3)_2\text{CHO}]_2\text{Ti}(\text{C}_6\text{H}_7\text{O}_2)_2$, Sigma Aldrich, 75 wt.% in 2-propanol) were used without further purification. The $\text{CH}_3\text{NH}_3\text{I}$ was prepared according to the reported procedure.¹ TiO_2 nanoparticles were synthesized following a previously reported method.^{2,3} To stabilize the as-obtained TiO_2 solutions, TiAcAc was added into the solution. The concentration of TiAcAc in TiO_2 solution is 15 $\mu\text{L}/\text{mL}$. The solution was saved in the refrigerator overnight before use.

Measurements

UV–Vis spectra were obtained with a Varian Cary 50 ultraviolet–visible spectrometer. XRD experiments were performed on a Panalytical X'Pert Pro X-ray Powder Diffractometer with Cu-K α radiation ($k = 1.5406 \text{ \AA}$). AFM was performed using Bruker Dimension 5000 Scanning Probe Microscope (SPM) in "tapping" mode. The SEM images were taken on a JEOL JSM-6700F. Steady-state photoluminescence was measured by Horiba Jobin Yvon system with an excitation at 650 nm. In the time-resolved PL measurement, the samples were excited by a pulsed laser (PDL 800-B system with an extended trigger) with a wavelength and frequency of 768 nm and 1MHz, respectively. The PL photons were counted by PicoHarp 300 after preamplification by PAM102. The Fermi level and HOMO level of the films were examined using ultraviolet photoelectron spectroscopy (UPS) (AXIS Ultra DLD). UPS spectra were acquired from He I (21.22 eV) excitation lines with sample biasing of 9 V.

Field-effect transistor (FET) device fabrication and characterization

To fabricate the device, 100 nm SiO₂ was thermally grown as a gate dielectric layer on the top of a heavily boron (p⁺⁺)-doped Si wafer. The substrates were sonicated with acetone and isopropyl alcohol, respectively. Then, substrates were treated by a ultra-violet (UV) irradiation for 20 min to eliminate organic substances and to improve wettability for the solution coating. The solution of DOR3T-TBDT was spin-coated on the substrate. The thickness is 100nm. The gold source and drain (S/D) electrodes (thickness = 85 nm) were deposited by thermal evaporation with a metal shadow mask. The channel region was defined with a width of 1000 μm and length of 100 μm (W/L). The electrical characteristics of the devices were measured in a dark box in ambient air using an Agilent 4155C semiconductor parameter analyzer. The parameter of TFTs was extracted from the conventional equations of TFT devices.

Conductivity test

Resistivity is measured by transmission line model (TLM). OTFT with different channel length are fabricated using the method mentioned above in the device fabrication part. Total resistance including the contact resistance and channel resistance is obtained by measuring output curve at zero gate bias. By plotting the total resistance against the channel length, sheet resistance of the channel is obtained and resistivity can be estimated assuming two-dimensional charge transportation.

Supporting pictures

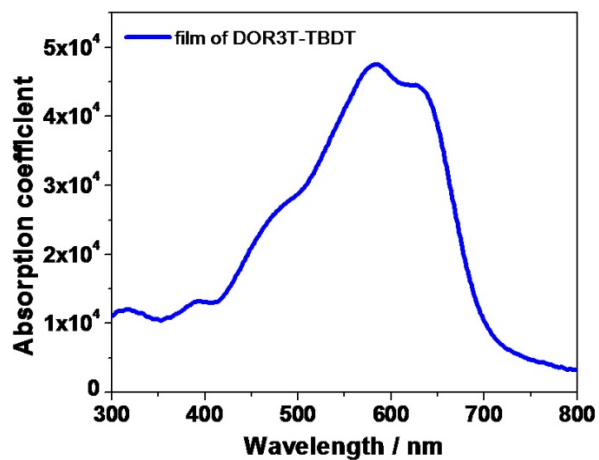


Figure S1. UV-Vis absorption spectrum of DOR3T-TBDT.

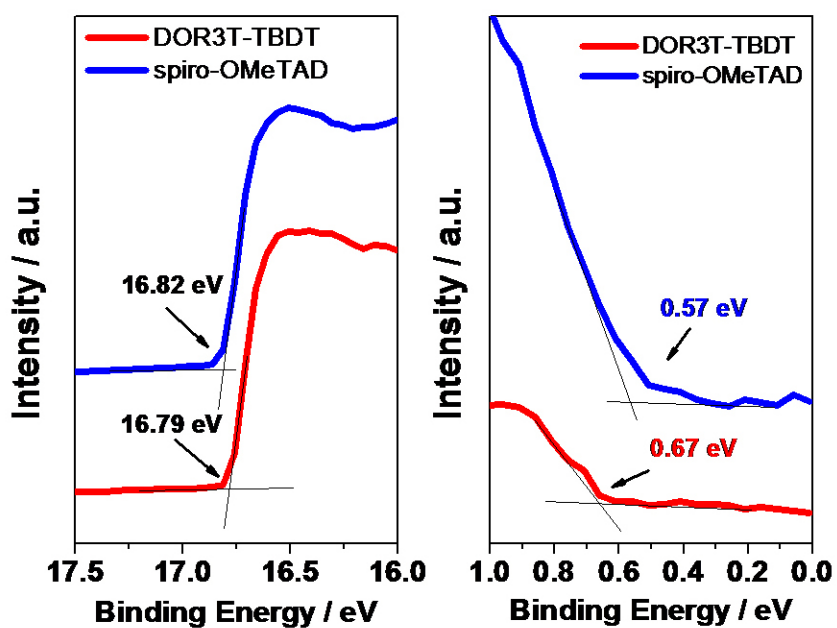


Figure S2. UPS spectra in the onset (right) and the cutoff (left) energy regions of the DOR3T-TBDT and spiro-OMeTAD film.

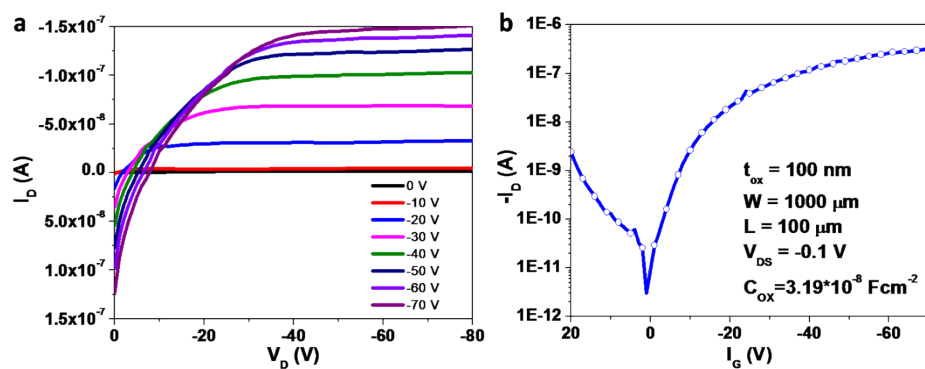


Figure S3. (a) Output characteristics for a DOR3T-TBDT based device with $L = 100 \mu\text{m}$ and $W = 1000 \mu\text{m}$. (b) Transfer characteristics of the same device.

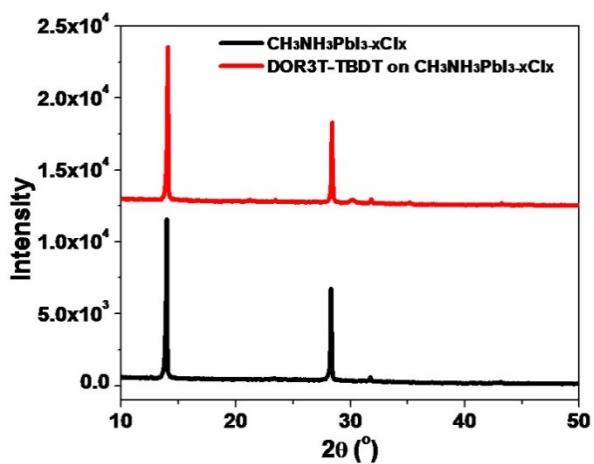


Figure S4. XRD patterns of perovskite films on glass/ TiO_2 substrate and DOR3T-TBDT film on glass/ TiO_2 /perovskite substrate.

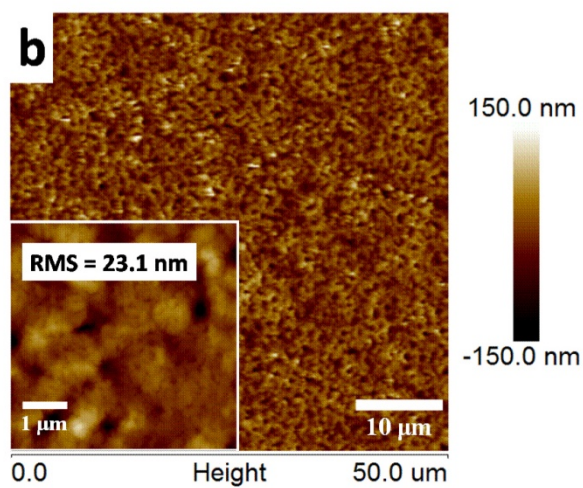
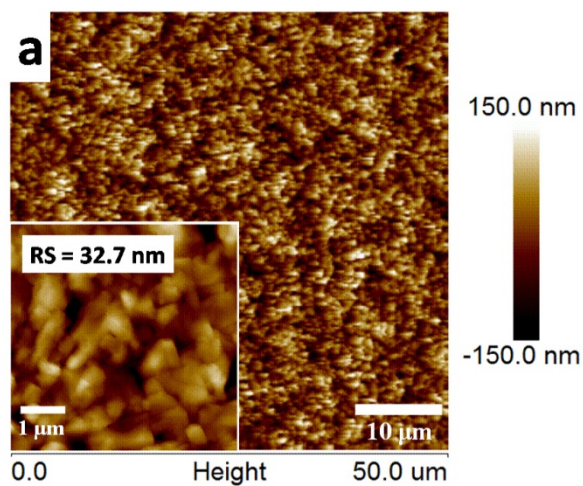


Figure S5. Surface morphology. Tapping-mode AFM height images ($50 \times 50 \mu\text{m}$) of (a) glass/ $\text{CH}_3\text{NH}_3\text{PbI}_{(3-X)}\text{Cl}_X$ and (b) glass/ $\text{CH}_3\text{NH}_3\text{PbI}_{(3-X)}\text{Cl}_X/\text{DOR3T-TBDT}$. Inset: the corresponding AFM height images ($5 \times 5 \mu\text{m}$).

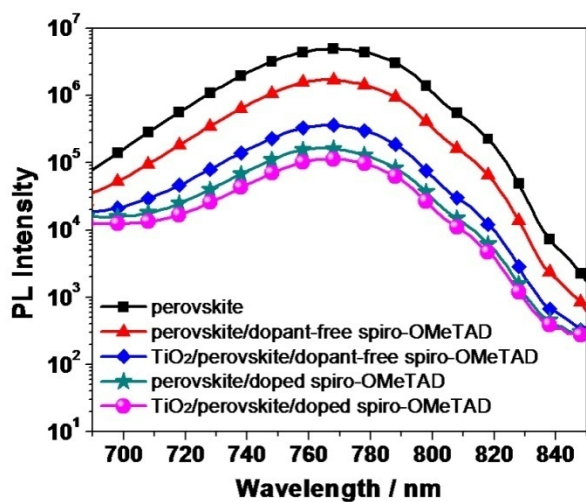


Figure S6. Photoluminescence spectroscopy. The steady-state PL spectra of glass/ $\text{CH}_3\text{NH}_3\text{PbI}_{(3-x)}\text{Cl}_x$, glass/ $\text{CH}_3\text{NH}_3\text{PbI}_{(3-x)}\text{Cl}_x$ /(dopant-free spiro-OMeTAD), glass/ TiO_2 / $\text{CH}_3\text{NH}_3\text{PbI}_{(3-x)}\text{Cl}_x$ /(dopant-free spiro-OMeTAD), glass/ $\text{CH}_3\text{NH}_3\text{PbI}_{(3-x)}\text{Cl}_x$ /(doped spiro-OMeTAD), and glass/ TiO_2 / $\text{CH}_3\text{NH}_3\text{PbI}_{(3-x)}\text{Cl}_x$ /(doped spiro-OMeTAD).

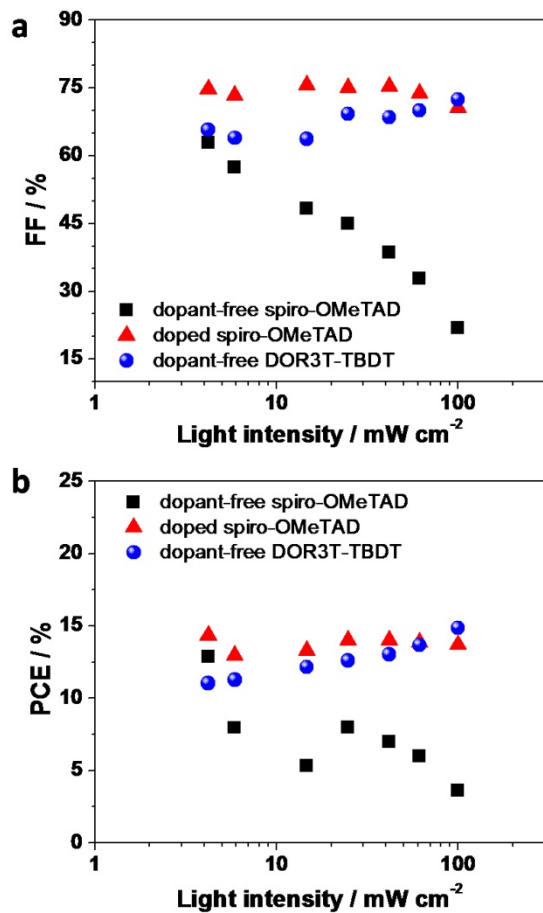


Figure S7. Perovskite solar cells using different HTLs under low light intensity (from 4.2 to 100 mW cm⁻², 0.042–1 Sun). (a) FF as a function of light intensity; (b) PCE as a function of light intensity.

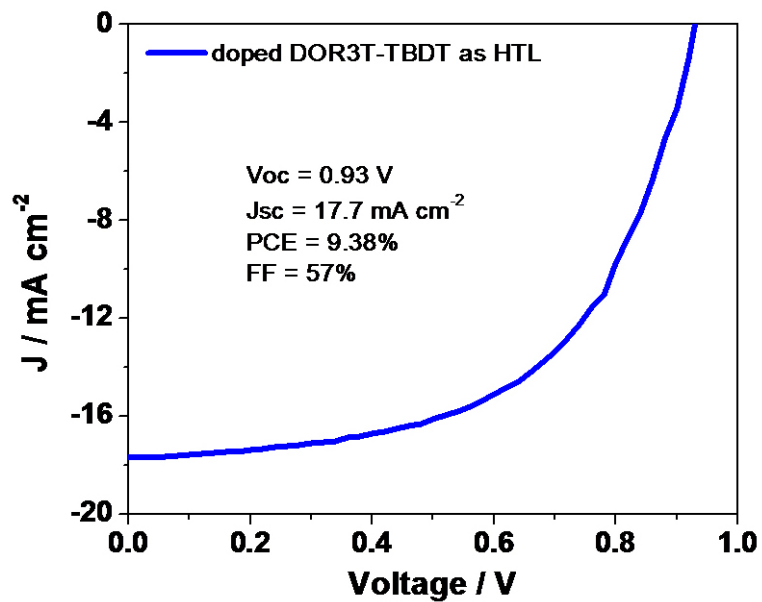


Figure S8. Device performance of perovskite solar cell using doped DOR3T-TBDT (DOR3T-TBDT + lithium bis(trifluoromethylsulfonyl)imide salt + tert-butylpyridine) as HTL.

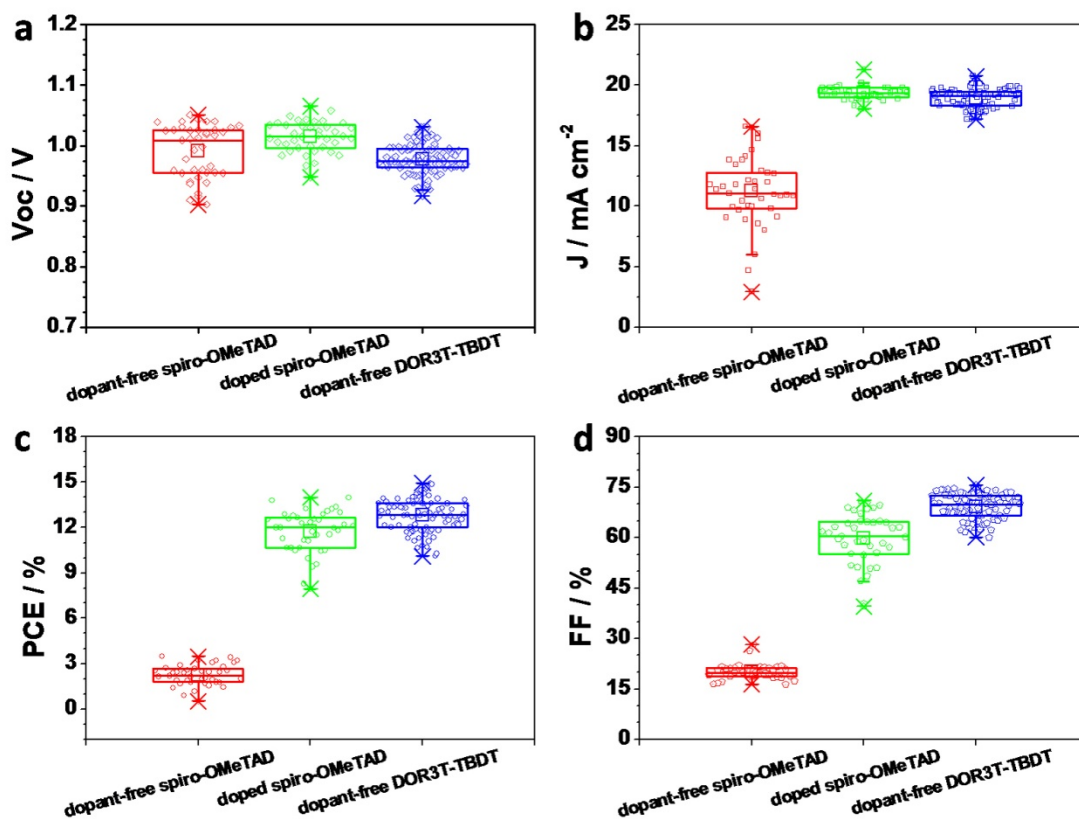


Figure S9. Perovskite solar cells performance variations by using different HTLs. Box chart of device parameters extracted from the current-voltage characteristic. Each point represents a single device. 40 devices for dopant-free or doped spiro-OMeTAD and 90 devices for dopant-free DOR3T-TBDT based cells.

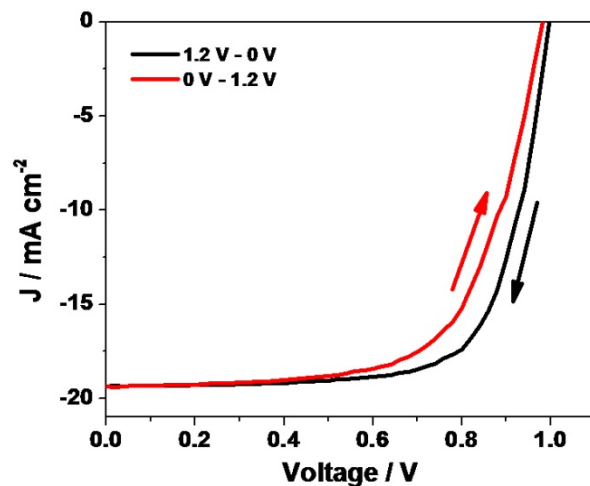


Figure S10. J-V curves of representative perovskite/dopant-free DOR3T-TBDT based device under different scan directions with bias step of 20 mV.

Table S1. Performance parameters of perovskite solar cells using different HTLs.

HTLs	dopant	J _{sc} (mA cm ⁻²)	Calculate J _{sc} (mA cm ⁻²)	Maximum EQE
Spiro-OMeTAD	without	16.6	15.2	66% (670 nm)
Spiro-OMeTAD	with	19.5	18.1	80% (510 nm)
DOR3T-TBDT	without	20.7	19.2	86% (480 nm)

Table S2. Representative perovskite/dopant-free DOR3T-TBDT based device under different scan directions.

HTLs	Scan directions	V _{oc} (V)	J _{sc} (mA cm ⁻²)	PCE (%)	FF (%)
dopant-free DOR3T-TBDT	reverse	1.00	19.37	13.97	72.1
	forward	0.98	19.38	12.44	65.5

References

- [1] M. M. Lee, J. Teuscher, T. Miyasaka, T. N. Murakami, H. J. Snaith, *Science* **2012**, 338, 643.
- [2] Wojciechowski, K.; Saliba, M.; Leijtens, T.; Abate, A.; Snaith, H. J. *Energy Environ. Sci.* **2014**, 7, 1142.
- [3] J. Wang, J. Polleux, J. Lim, B. Dunn, *J. Phys. Chem. C* **2007**, 111, 14925.